



ACT Project Number:  
**271498**

Project acronym:  
**ELEGANCY**

Project full title:  
**Enabling a Low-Carbon Economy via Hydrogen and CCS**

**ERA-Net ACT project**

Starting date: 2017-08-31  
Duration: 36 months

**D2.3.4**  
**Experimental observations of single and multiphase flows on carbonates**

**Actual Delivery date: 2019-07-10**

Organization name of lead participant for this deliverable:  
**Imperial College London**

<b>ACT ELEGANCY, Project No 271498, has received funding from DETEC (CH), BMWi (DE), RVO (NL), Gassnova (NO), BEIS (UK) and Gassco, Equinor and Total, and is cofunded by the European Commission under the Horizon 2020 programme, ACT Grant Agreement No 691712.</b>		
<b>Dissemination Level</b>		
<b>PU</b>	Public	X
<b>CO</b>	Confidential , only for members of the consortium (including the Commission Services)	



<b>Deliverable number:</b>	D2.3.4
<b>Deliverable title:</b>	Document reporting results of equilibrium and dissolution multi-phase core-flooding experiments
<b>Work package:</b>	WP 2 CO <sub>2</sub> transport, injection and storage
<b>Lead participant:</b>	ICL

<b>Authors</b>		
<b>Name</b>	<b>Organisation</b>	<b>E-mail</b>
Ronny Pini*	ICL	r.pini@imperial.ac.uk
Sam Krevor	ICL	s.krevor@imperial.ac.uk
Swapna Rabha	ICL	s.rabha@imperial.ac.uk
Sojwal Manoorkar	ICL	s.manoorkar@imperial.ac.uk

\*Mark Lead author with asterisk

<b>Keywords</b>
Petrophysics, core-analysis, chemical transport, multiphase flow

<b>Abstract</b>
<p>Capillary and solubility trapping are considered two key storage mechanisms in geologic carbon sequestration applications. Decreasing the uncertainty associated with predictive modelling of these two trapping processes remains challenging, because the effects of heterogeneity at sub-seismic resolution are not well understood. Within ELEGANCY, laboratory experiments are carried out to quantify the impact of small-scale heterogeneity on CO<sub>2</sub> trapping in laboratory rock cores. In this report, results from both single- and two-phase flow experiments in two carbonate rock samples are presented. At the core of the experimental approach is the use of two multi-dimensional imaging techniques, namely X-ray Computed Tomography and Positron Emission Tomography, to provide precise measurements of gas saturation and solute concentration within the sample, non-invasively. It is shown that subcore-scale heterogeneities have a major impact on both the transport and two-phase flow properties of the rocks, which is manifested through a characteristic dependence on the experimental flow rate. These experimental observations represent an essential input for the calibration of numerical models that can be used to predict trapping processes at conditions prevalent in the subsurface.</p>



## TABLE OF CONTENTS

	Page
1. INTRODUCTION.....	7
2. MATERIAL SELECTION AND CHARACTERIZATION .....	8
3. EXPERIMENTAL SETUP AND TECHNIQUES .....	10
Single phase tracer test.....	10
Multiphase and relative permeability test .....	11
4. RESULTS.....	13
Single phase tracer test.....	13
Multiphase and relative permeability test .....	16
5. CONCLUDING REMARKS .....	18
6. REFERENCE .....	19



## 1. INTRODUCTION

Flow and transport in rocks with or without fractures plays an important role in many scientific fields ranging from groundwater contamination, oil recovery and geologic carbon sequestration (GCS). ELEGANCY focuses on the latter by providing laboratory observations supported by numerical modelling to shed light on the physics of the CO<sub>2</sub>-brine displacement.

Estimates of storage potential in subsurface reservoirs rely on the effectiveness of a number of chemical and physical processes that act towards retaining the CO<sub>2</sub> in the host reservoir. In the long-term, the focus of storage security is expected to shift to two trapping mechanisms, capillary and solubility trapping, which can immobilize a significant portion of the buoyant and mobile CO<sub>2</sub> plume. Capillary trapping refers to the presence in the pore space of the rock of a disconnected CO<sub>2</sub>-rich phase and is largely affected by the interplay between drainage and imbibition processes. The dissolution of the trapped CO<sub>2</sub> into reservoir brines and the subsequent mixing of the CO<sub>2</sub>-rich solution with fresh brine is another key mechanism towards the long-term immobilization of the buoyant CO<sub>2</sub> plume. A key question here relates to the estimation of effective rates of dissolution and dilution.

Because geological formations are inherently heterogeneous, decreasing the uncertainty associated with predictive modelling of the flow and trapping of the injected CO<sub>2</sub> remains a key R&D need. In particular, new approaches are needed to characterize the impact of rock heterogeneity at sub-seismic resolution on the movement and trapping of the injected CO<sub>2</sub>, including the presence of fractures. Such approaches include the deployment of core-analysis workflows that incorporate novel imaging technology for direct observations of fluid distribution. Outcomes from these studies are properties for CO<sub>2</sub> relative permeability, trapping and transport that reflect the impact of small-scale heterogeneity.

Within ELEGANCY, a laboratory experimental campaign has been designed to address the above-mentioned issues on heterogeneous carbonate rocks. In this report, we present and discuss results from both single-phase (transport) and two-phase flow experiments aimed at revealing the impact of heterogeneities on the CO<sub>2</sub>/water displacement, trapping and the subsequent mixing of the CO<sub>2</sub>-rich brine in carbonate rocks.

## 2. MATERIAL SELECTION AND CHARACTERIZATION

Two carbonate core samples were used, namely a 2 inches-diameter Ketton Limestone core (KL, Ketton Quarry, Rutland, UK) and a 1.5 inches-diameter Indiana Limestone core (IL, Salem Formations, Indiana). Photographs of the two samples are shown in Figure 1.

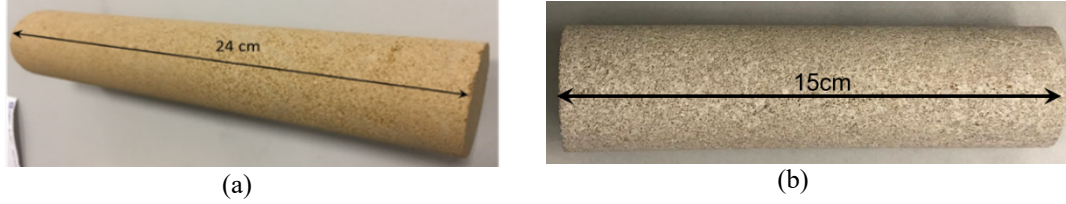


Figure 1. Photographs of the Ketton Limestone core (length = 24 cm, diameter = 4.7 cm) and Indiana Limestone core (length = 15 cm, diameter = 3.8 cm).

KL is composed of smooth spherical grains with average particle diameter  $\sim 0.6$  mm and is mono-mineralic (99%  $\text{CaCO}_3$ ), whereas IL is a calcite-cemented grain-stone made up of fossil fragments and oolites. The measured porosity and permeability of both core samples are reported in Table 1.

Table 1: Porosity and absolute permeability of the core samples

	Indiana	Ketton
Porosity (-)	0.17	0.2348
Absolute permeability (mD)	24	2000

The distribution of porosity within the samples was measured by X-ray CT by combining scans acquired under dry- and water-saturated conditions and using the following equation:

$$\phi = \frac{\overline{CT}_{\text{wet}} - \overline{CT}_{\text{dry}}}{CT_{\text{water}} - CT_{\text{air}}} \quad (\text{Eq 1})$$

where  $\overline{CT}_{\text{wet}}$  and  $\overline{CT}_{\text{dry}}$  refer to the measurements of the dry- and water-saturated sample, while the denominator represents a normalization with the CT numbers of the pure fluids, which have been obtained from a calibration of the scanning instruments ( $CT_{\text{water}} - CT_{\text{air}} = 899$  HU [Joss and Pini, 2017]). The two-dimensional porosity distribution along the central longitudinal plane is shown in Figure 2(a) and (b), for IL and KL, respectively.



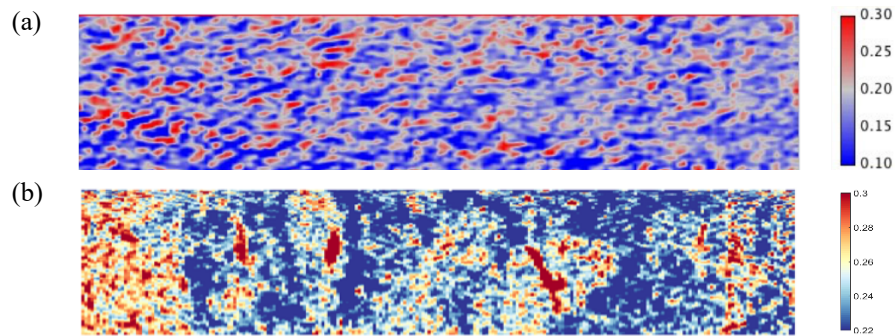


Figure 2. Porosity map of the central vertical plane of samples of (a) Indiana Limestone and (b) Ketton Limestone. The dimensions of the samples are reported in Table 1.

The slice-averaged porosity along the length of each core sample were also calculated using Eq 1 (using slice-averaged CT numbers) and are shown in Figure 3. The samples depict different types and scale of heterogeneity. It can be seen that KL shows a more pronounced degree of porosity variation along the core as compared to IL, which shows a rather flat porosity profile.

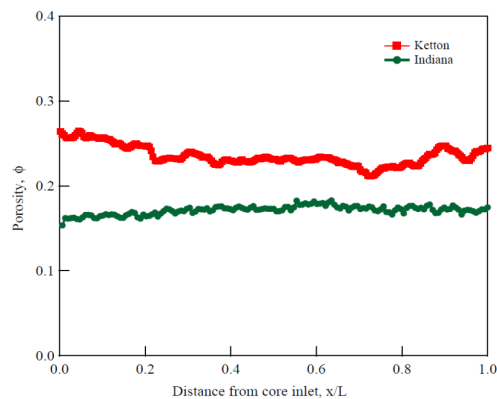


Figure 3. Porosity profile along the length of the carbonate samples.

### 3. EXPERIMENTAL SETUP AND TECHNIQUES

#### Single phase tracer test

The in-house developed core-flooding apparatus used in this work is shown in Figure 4. It consists of an aluminum core holder that accommodates a cylindrical sample of diameter up to 5 cm and of variable length (10 – 40 cm). The sample is positioned between a fixed end cap (downstream) and an adjustable end cap (upstream). Both end caps have multiple ports for fluid flow and pressure measurements. A differential pressure transducer (DPI, Keller UK, model PRD-33X, accuracy: 0.05%FS) is connected at the upstream and downstream of the core holder. Another differential pressure is connected at the downstream and other end is open to atmosphere. A constant confining pressure is maintained between the jacketed core sample and outer aluminum tube by a high-pressure syringe pump (Teledyne ISCO, 500D).

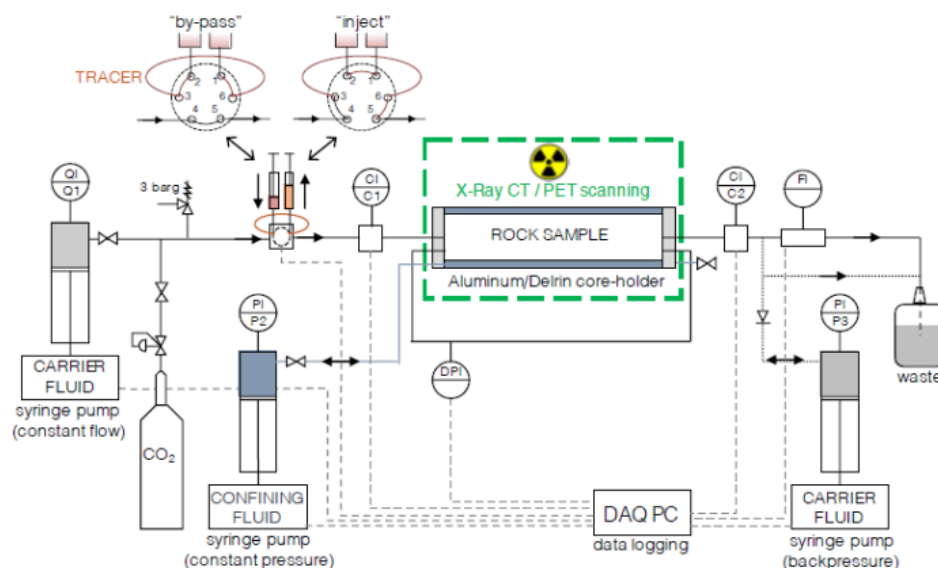


Figure 4. Schematic diagram of the experimental core-flooding apparatus installed at Imperial College London, London, United Kingdom (Kurotori et al. 2019)

The faces of the two end-caps are covered with a circular aluminum mesh of the same diameter (aperture size of 0.085 mm, Advent Research Materials Ltd, UK) before sliding a heat-shrink FEP sleeve (50.8 mm bore, Polyon 200 Technology Ltd, UK) on to the core sample and to the two end-caps. The shrink sleeve is carefully heated to get a tight annular seal around the sample and the end caps. After assembling the core holder, the annular space between the core sample and the aluminium cylinder is filled with confining fluid (tap water) while maintaining the core-holder in vertical position to remove all the air present in the system. The confining pressure is increased gradually to the set value. In this work, a confining pressure of 20 bar is used for the single-phase tracer tests.

After setting the confining pressure, the core holder is placed horizontally on the bed of the Medical X-ray CT instrument (Aquilion, TSX-101A, Toshiba Medical Systems Corporation) hosted in the Multiscale Imaging Laboratory at Imperial College London (Figure 5). Prior to

the start of the experiment, CO<sub>2</sub> is purged in to the core to flush any air present in the core sample. The aqueous carrier solution is then circulated into the core for at least 8 pore volumes (PV) to achieve complete liquid saturation of the pore space. Potassium chloride (KCl, > 99%, Sigma Aldrich) and potassium iodide (KI, ReagentPlus R, 99%, Sigma Aldrich) are used to prepare aqueous neutrally buoyant carrier (KCl, 7.0wt%) and tracer (KI, 6.1wt%) solutions. The details of the experimental procedure are reported in Kurotori et al. 2019. The tracer concentration of the inflow and outflow solutions are measured by two conductivity micro flow cells (CI, Model 829, Amber Science, USA) mounted at up- and down-stream of the core-holder. The experiments are carried out at 20°C and 0.1 MPa.

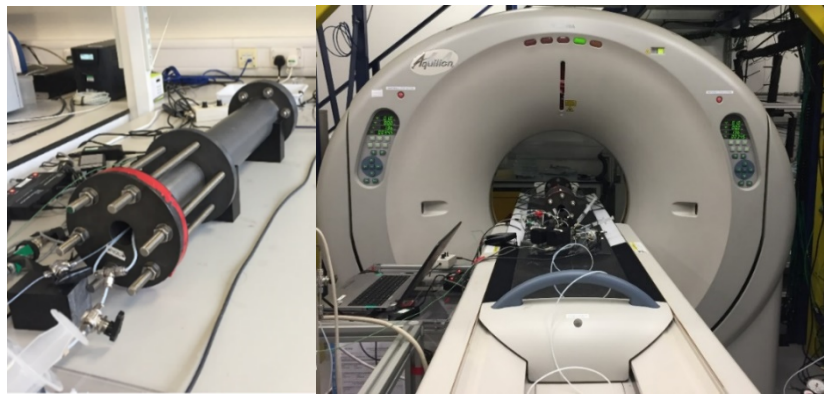


Figure 5. Medical X-ray Computed Tomography scanning instrument available at Imperial college London, UK with the core holder used in this study.

### Multiphase and relative permeability test

The drainage core-flooding experiments is performed in a high pressure, high temperature closed flow rig (Figure 6). Two dual high-pressure syringe pumps for N<sub>2</sub> and DI water are used to co-inject the fluids. Automatic valves for each pair of pumps control the fluid flow and refill the pumps to maintain the continuous circulation of fluids through the core. A two-phase separator is used to separate the fluid phases leaving the sample. The fluids are returned to the pumps from the separator via a water return line connected to the base of the separator and a N<sub>2</sub> return line connected to the top of the separator. The rock sample is placed inside the aluminium core holder in horizontal orientation to minimize the gravity effect. A back-pressure pump at the outlet side is used to maintain the system pressure and another pump is used to maintain the confining pressure 4MPa above the experimental pressure. Pressure is measured at inlet and outlet face of the core using high accuracy transducers. All flow lines and pumps are constructed from a corrosion resistant alloy (Hastelloy). The core holder is fixed inside a CT-scanner so that core can be moved during the scans. Fluid saturations are measured using medical X-ray CT-scanner using voltage of 120kV, current of 200 mA and exposure time of 1 s. Scans of 1mm thickness are taken for the entire length of the core, with a x-y resolution of 512 pixels or 170 μm which gives voxel dimension of about (0.17 x 0.17 x 1) mm<sup>3</sup>.

The experiments are carried out at 20°C and 10MPa under which N<sub>2</sub> is in the supercritical condition. The drainage cycle is performed in which the core is saturated with water at the start of the experiment. The nitrogen fractional flow rate is increased by keeping a constant total

flow rate. The relative permeability of each phase is computed by using the extended Darcy's law for multiphase flow (Eq 2), while fluid saturation is obtained by combining three sets of CT images (Eq 3).

$$k_{r,i}(S_i) = \frac{q \mu_i L}{A K \Delta P} \quad (\text{Eq 2})$$

$$S_{N2} = \frac{\overline{CT}_{exp} - \overline{CT}_{wet}}{\overline{CT}_{N2} - \overline{CT}_{wet}} \quad (\text{Eq 3})$$

In the same experiment, residual saturation is obtained by carrying out imbibition at the end of drainage cycle.

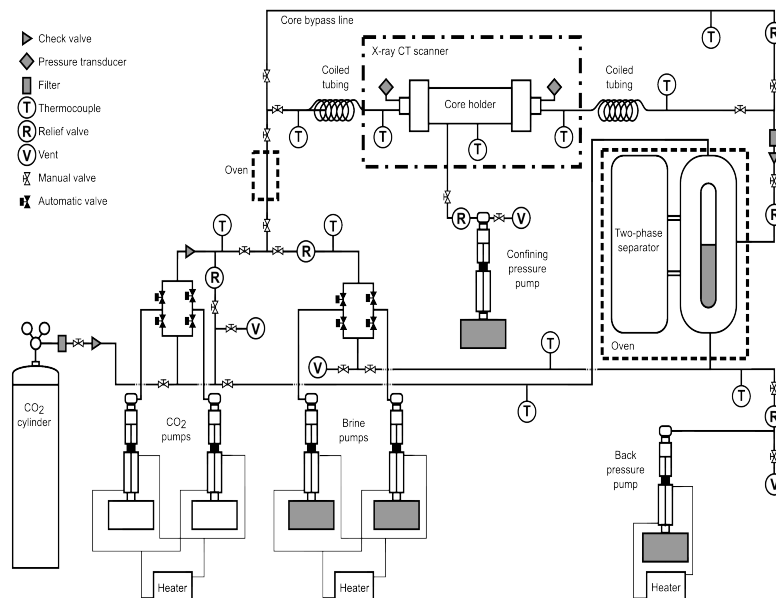


Figure 6. Schematic diagram of the experimental core-flooding rig used for relative permeability measurement (Reynolds, 2016)

## 4. RESULTS

### Single phase tracer test

The flows rates, confining pressure, tracer volume and Peclet number applied for the tracer experiments on Ketton Limestone are reported in Table 2.

Table 2: Operating parameters considered in the experimental campaign

Flowrate (mL/min)	Confining pressure (Bar)	Tracer volume (ml)	Pe* ( $\frac{vL}{D}$ )
2, 4, 8, 10, 15	20	2	71, 143, 286, 358, 537

where  $v$  is the pore fluid velocity,  $D$  is the molecular diffusion coefficient ( $1 \times 10^{-9}$  m<sup>2</sup>/s) and  $l$  is the characteristic length (In this study, the mean grain diameter of the rock sample is considered as the characteristic length, which is 600  $\mu$ m for Ketton Limestone). The breakthrough curves measured from the tracer tests on the Ketton core sample at different flow rate are shown in Figure 7, while the corresponding mean residence times are reported in Table 3. The experimental mean residence time is obtained from the first moment of the residence time distribution function [Kurotori et al. (2019)]:

$$\tau_{\text{exp}} = \int_0^{\infty} tE(t)dt \quad (\text{Eq 4})$$

where,  $\tau_{\text{exp}}$  is the mean residence time calculated from the experiment and  $E(t)$  is the residence time distribution function. The theoretical mean residence time is calculated as

$$\tau = \phi AL/q \quad (\text{Eq 5})$$

where  $\phi$  is the measured mean porosity of the sample,  $A$  is the cross-sectional area,  $L$  is the length of the core and  $q$  is the flow rate.

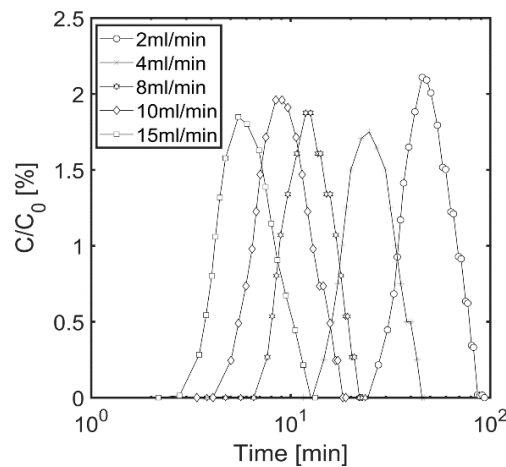


Figure 7. Breakthrough curves measured from the tracer tests on Ketton Limestone

For all the flow rates, the experimental mean residence time is found to be higher than the theoretical value. Because the microporosity present in the Ketton Limestone is not included in the theoretical calculations, this observation suggests that (i) a fraction of this microporosity is accessed by the tracer and that (ii) the level of accessibility depends on the flow rate.

Table 3. Mean residence time of the solute as a function of flow rate

Flow rate (ml/min)	Mean residence time (min)	
	Theoretical	Experiments
2	48.717	53.722
4	24.356	27.468
8	12.179	13.634
10	9.743	10.453
15	5.5518	6.913

In the following, we investigate the role of subcore-scale heterogeneity in controlling the transport of solute within the sample. As depicted in Figure 8 (a), a workflow has been developed that combines observations of chemical transport by Positron Emission Tomography (PET) with solution from numerical simulations using CrunchFlow [Steeffel et al., 2014]. For the latter, a 2D domain is built based on the measured porosity distribution (obtained by X-ray CT) and the associated permeability values estimated from two different methods. The first one produces a permeability map using a porosity-based model [Benson et al., 2009], while the second uses the gas saturation map to identify regions of high- and low-permeability using a thresholding method (large gas saturations corresponds to high permeability). Figure 8(b) shows a comparison between the measured and the predicted tracer plume. We note that the experimental results correspond to previously published data [Kurotori, 2019] on a KL core sample of length = 10 cm and diameter of 5 cm at a flow rate of 4 ml/min. For the numerical simulations, the following parameter were used: core-averaged porosity of 0.23, molecular diffusion coefficient of  $1 \times 10^{-9}$  m<sup>2</sup>/sec, tracer concentration of  $6 \times 10^{-11}$  mol/kgw (corresponding to 0.556 mCi/ml) and injected tracer volume of 1 ml. As shown in Figure 8 (b), the predicted result based on gas saturation-based permeability map (bottom panel) reproduce more closely the characteristic spreading of the solute caused by subcore scale heterogeneity, as opposed to the model-based simulation results where the solute plume remains largely unaffected. This workflow will be used for the longer sample considered in this report to further analyze additional spatial measures of mixing, such as the scalar dissipation and the dilution index.

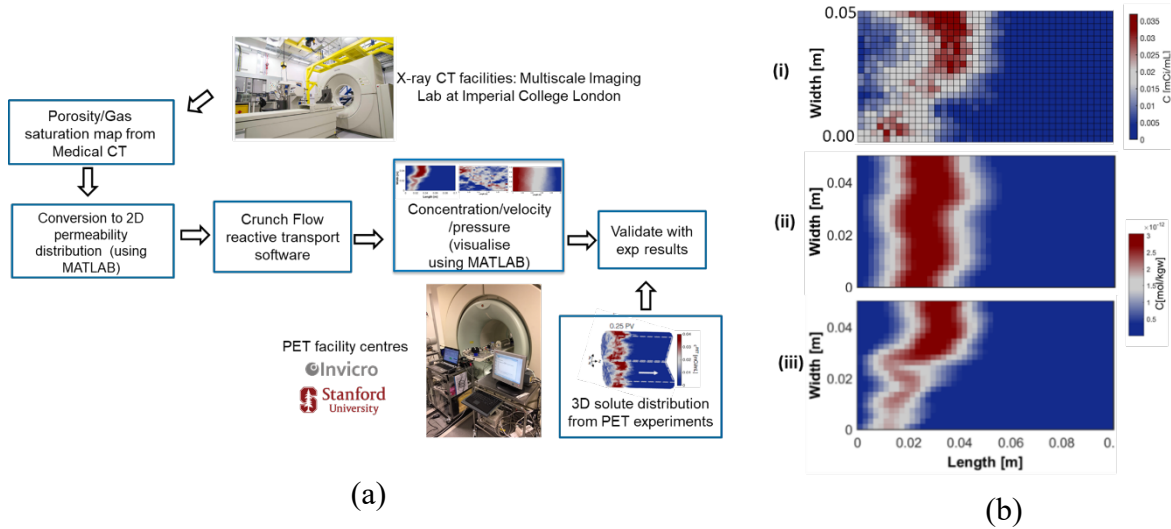


Figure 8 (a) Methodology used in this work, (b) Tracer concentration profile after injecting 0.3 pore volumes (i) Experimental results captured by Positron emission tomography [Kurotori et al., 2019]; (ii) Predicted results using porosity-based model [Benson et al., 2009] and (iii) Predicted results based on thresholding of gas saturation maps.



### Multiphase and relative permeability test

The drainage experiments are carried out for two total flow rates, 0.5 ml/min and 5 ml/min. At low flow rate (0.5 ml/min), capillary forces dominate the flow, whereas at high flow rate (5 ml/min), the flow is controlled by viscous forces. The relative permeability curves of IL are shown in Figure 9 (a). At the start of the drainage experiments, the core is fully saturated with water and fractional flow of nitrogen is increased, while maintaining a constant total flow rate. The liquid permeability ( $k_{r,w}$ ) decreases and the gas permeability ( $k_{r,nw}$ ) increases as the water saturation decreases. The relative permeability curve for high flow rate is very different from the low flow rate permeability. The strong flow rate dependence of the relative permeability is the result of the heterogeneities in the core. The millimetre scale heterogeneities in the samples (as shown in Figure 3) dominate the fluid distribution in pore spaces at low capillary number.

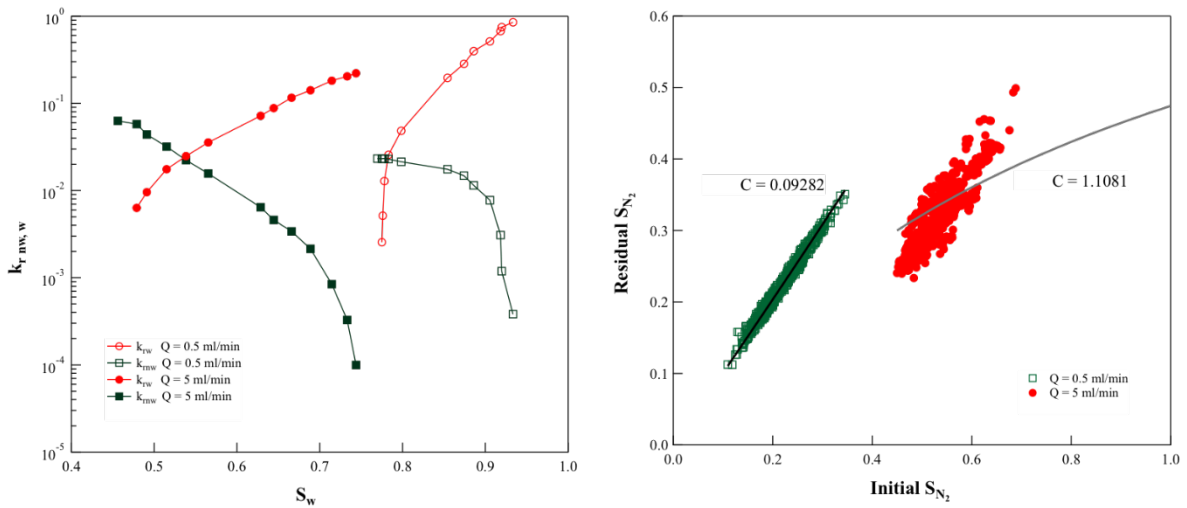


Figure 9 (a) Relative permeability in Indian core at two flow rates, (b) Residual trapping in Indiana core at two flow rates.

The initial (at the end of the drainage cycle) and residual (at the end of the imbibition cycle) nitrogen saturation profiles along the length of core at 0.5 ml/min and 5 ml/min are shown in Figure 10. At low flow rate, the residual saturation is lower than at high flow rate experiment, but a higher degree of trapping is observed. The latter is quantified through the Initial-Residual plot shown in Figure 9(b), where the data have been parameterized using the Land model Residual (Eq 5).

$$S_{N_2,r} = \frac{S_{N_2,i}}{1 + C S_{N_2,i}} \quad (\text{Eq 5})$$

The coefficient  $C$  is obtained by fitting the Land equation through the points. A lower value of  $C$  suggests more trapping of non-wetting phase. The extent of trapping for low flow rate experiments is higher where heterogeneities dominate the flow properties of the rock.



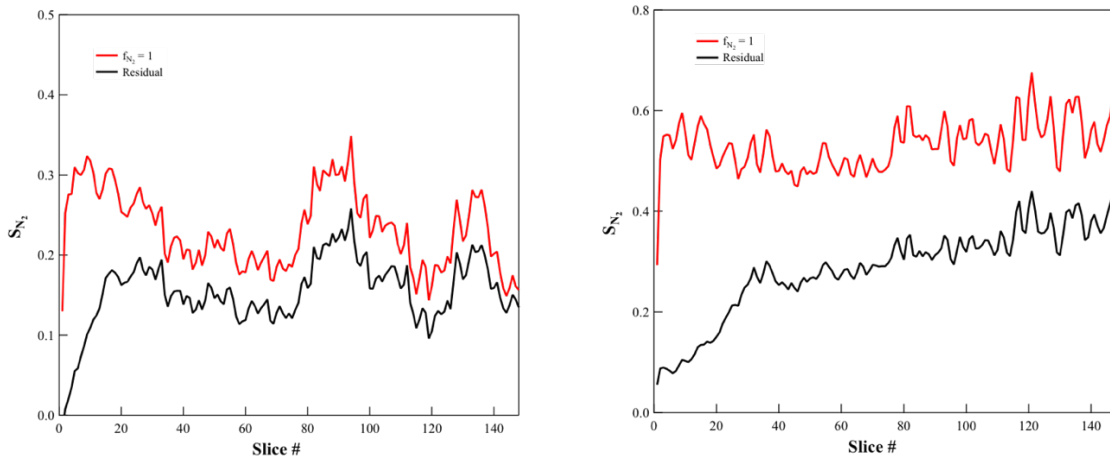


Figure 10 (a) Initial and residual nitrogen saturation along the core for 0.5 ml/min (b) Initial and residual nitrogen saturation along the core for 5 ml/min

## 5. CONCLUDING REMARKS

In this report, results from an experimental campaign have been presented, where the single- and two-phase flow properties of two carbonate rocks have been measured.

The single-phase tracer experiments were performed on a Ketton Limestone core by measuring tracer breakthrough curves in the range of Péclet numbers  $71 \leq Pe \leq 537$ . A numerical model was developed to analyze the effects of spatial heterogeneities in controlling the tracer migration within the sample. To this aim, a new approach to estimate the distribution of small-scale permeability heterogeneities was developed that uses a thresholding method based on observed gas saturation levels. The comparison with direct observations of tracer distribution by Positron Emission Tomography (PET) showed that this approach provides a better agreement as compared to a porosity-based model.

Measurements of relative permeability and trapping characteristics were carried out on an Indiana Limestone at two different flow rates. A strong dependency of the two multi-phase properties on the flow rate was observed, this being the result of the presence of subcore-scale heterogeneities. In particular, it was observed that heterogeneity results in increased trapping, as quantified by the trapping coefficient of the Land model.

## 6. REFERENCE

Joss, L. and Pini, R. (2017) Digital Adsorption: 3D Imaging of Gas Adsorption Isotherms by X-ray Computed Tomography *J. Phys. Chem. C* 2017, 121, 48, 26903-26915.

Kurotori, T., Zahasky, C., Hejazia, S. A., Shah, S. M., Benson, S. M., and Pini, R. (2019) Measuring, Imaging and Modelling Solute Transport in a Microporous Limestone. *Chemical Engineering Science*. 196, 366-383.

Reynolds C. A. (2016) Two-phase flow behaviour and relative permeability between CO<sub>2</sub> and Brine in sandstones at the pore and core scales. PhD thesis, Imperial College London, London, UK.

Steeffel, C., Appelo, C. A., Arora, B., D, J., Kalbacher, T., O, K., . . . Yeh, G. T. (2014). Reactive transport codes for subsurface environmental simulation. *Computational Geosciences*, 19(3), 445-478.

Benson, S.M., Perrin J.-C., Krause, M., Kuo, C.-W., and Esposito, A. (2009) Annual Report, Global climate and energy project. Stanford University, Stanford, California.